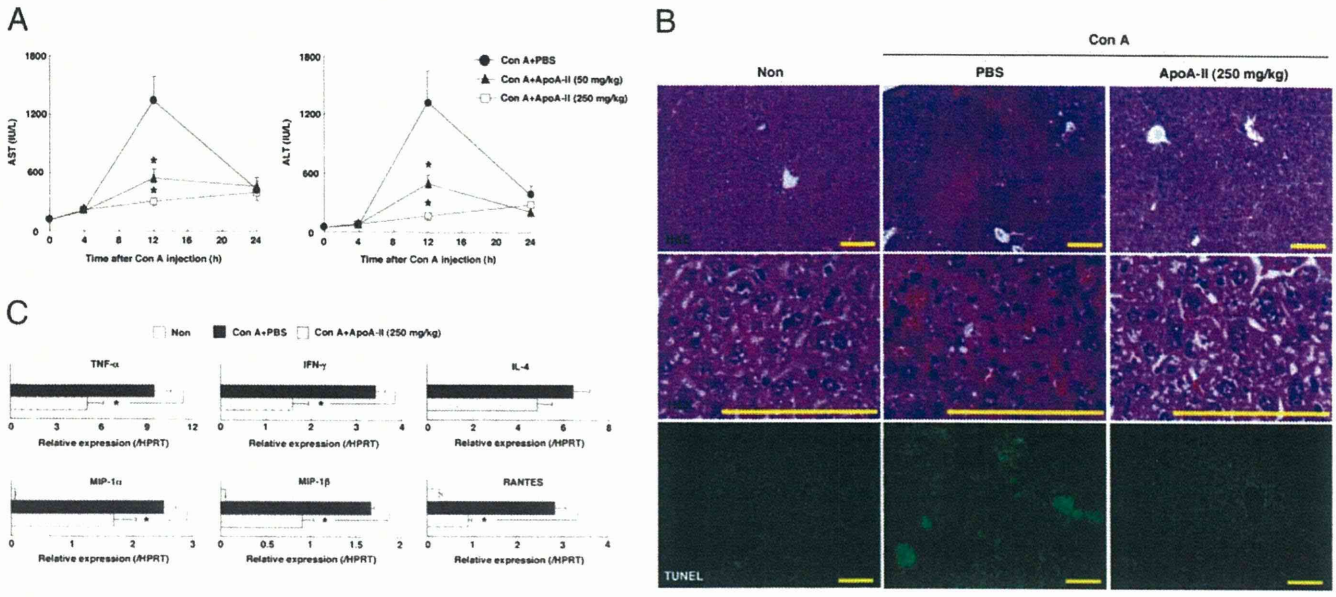

FIGURE 2. Attenuation of Con A-induced hepatitis by ApoA-II administration. *A*, Plasma AST and ALT levels in Con A-induced hepatitis in mice. Con A (12.5 mg/kg, i.v.) and vehicle (PBS, i.v.) or Con A and ApoA-II (50 or 250 mg/kg, i.v.) were injected into BALB/c mice. The plasma was collected 4, 12, and 24 h after Con A injection. The results are expressed as mean ± SD (n = 8). *$p < 0.05$, compared with PBS-administered mice. *B*, Livers were collected 12 h after Con A injection, and liver damage was evaluated by H&E and TUNEL staining. Scale bars, 100 μm (*top* and *middle panels*, H&E staining) and 50 μm (*bottom panels*, TUNEL staining). *C*, Quantitative RT-PCR analysis for TNF-α, IFN-γ, IL-4, MIP-1α, MIP-1β, and RANTES mRNA expression in the liver tissue was measured 12 h after Con A injection and expressed as a ratio to HPRT. The results are expressed as mean ± SD (n = 3). *$p < 0.05$, compared with PBS-administered mice.

addition of ApoA-II. Increased phosphorylation of c-Jun was detected 3 h after Con A stimulation and was inhibited by ApoA-II but not ApoA-I. The phosphorylation of IκBα, an indicator of the activation of the NF-κB signaling pathway, was not affected by the addition of ApoA-II. We did not detect any increase in the phosphorylation of p38 MAPK after Con A stimulation. The nuclear translocation of NFATc1 was detected 5 min after Con A stimulation and was significantly inhibited by the addition of

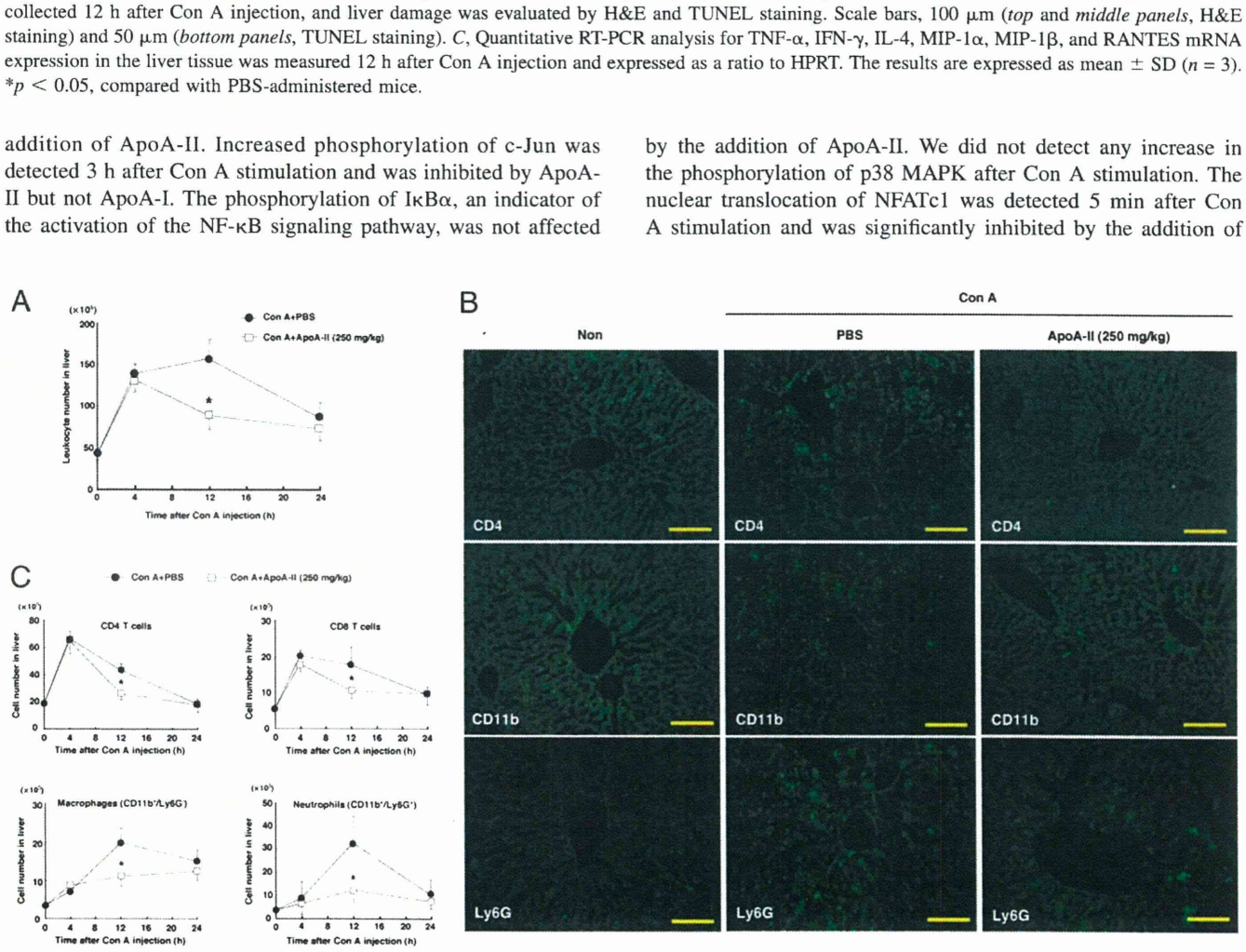

FIGURE 3. Suppression of Con A-induced leukocyte infiltration into the liver by ApoA-II administration. *A*, Total leukocyte cell numbers in the liver. Con A (12.5 mg/kg, i.v.) and vehicle (PBS, i.v.) or Con A and ApoA-II (250 mg/kg, i.v.) were administered into BALB/c mice. Livers were collected 4, 12, and 24 h after Con A injection. The results are expressed as mean ± SD (n = 8). *$p < 0.05$, compared with PBS-administered mice. *B*, Livers were collected 12 h after Con A injection, and leukocyte migration into the liver was evaluated by staining with Abs specific for CD4, CD11b, and Ly6G. Scale bars, 50 μm. *C*, Flow cytometric analysis of leukocytes migrated in the liver was performed. The results are expressed as mean ± SD (n = 8). *$p < 0.05$, compared with PBS-administered mice.

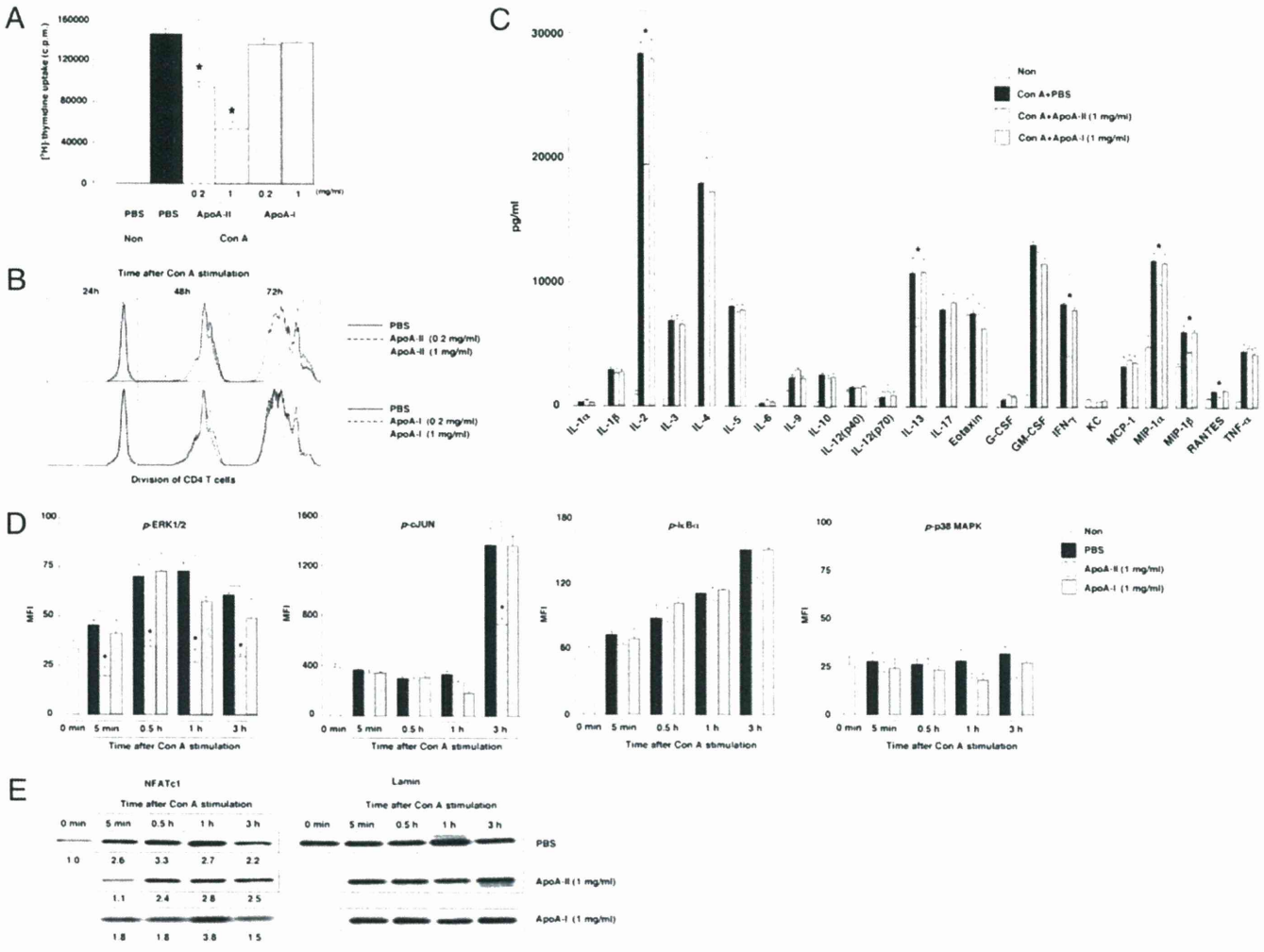

FIGURE 4. Suppression of the activation and function of mouse CD4 T cells. *A*, The proliferative response of mouse CD4 T cells was determined by [^{3}H]thymidine uptake. Purified splenic CD4 T cells were stimulated with Con A (5 μg/ml) for 40 h in the presence of ApoA-II or ApoA-I (0.2 or 1 mg/ml). The results are expressed as mean ± SD ($n = 5$). *$p < 0.05$, compared with PBS-added CD4 T cells. *B*, Purified splenic CD4 T cells were labeled with CFSE and stimulated with Con A in the presence of ApoA-II or ApoA-I. *C*, Purified splenic CD4 T cells were stimulated with Con A for 24 h in the presence of ApoA-II or ApoA-I, and the amounts of 23 cytokines in the culture supernatant were assessed by Bio-Plex. The results are expressed as mean ± SD ($n = 5$). *$p < 0.05$, compared with PBS-added CD4 T cells. *D*, The expression of signaling molecules was assessed by Bio-Plex. The results are expressed as mean ± SD ($n = 5$). *$p < 0.05$, compared with PBS-added CD4 T cells. *E*, The protein expression of NFATc1 or lamin in the nuclear fraction of CD4 T cells stimulated with Con A in the presence of ApoA-II or ApoA-I was assessed. Arbitrary densitometric units were calculated by dividing the density of NFATc1 by the density of lamin and are shown under each indicated time point for the NFATc1 band. Similar data were obtained from three independent experiments.

ApoA-II (Fig. 4*E*). In contrast, ApoA-I had very little effect on the activation of signaling molecules. These results indicate that ApoA-II suppresses the activation and function of mouse CD4 T cells by inhibiting the ERK–MAPK pathway and NFAT signaling pathway activated by Con A stimulation.

Suppression of the activation of human CD4 T cells by ApoA-II

Next, we examined whether ApoA-II suppressed the activation of human CD4 T cells. As shown in Fig. 5*A*, ApoA-II, but not ApoA-I, significantly suppressed [^{3}H]thymidine uptake by Con A-stimulated human CD4 T cells. The rate of cell division of Con A-stimulated human CD4 T cells was also suppressed by the addition of ApoA-II but not ApoA-I (Fig. 5*B*). In addition, we examined the effect of ApoA-II on the production of cytokines and chemokines by human CD4 T cells stimulated with Con A (Fig. 5*C*). Among the cytokines and chemokines tested, the production of IL-2, IL-9, IL-10, IL-17, IFN-γ, IFN-γ–inducible protein 10, and MIP-1α were significantly suppressed by ApoA-II. Again, no effect was observed by ApoA-I. These results indicate that ApoA-II suppressed the activation of Con A-stimulated human CD4 T cells.

Exacerbation of Con A-induced hepatitis in ApoA-II$^{-/-}$ mice

We examined the physiological roles of ApoA-II in Con A-induced hepatitis using ApoA-II$^{-/-}$ mice. No spontaneous pathological AST and ALT levels or leukocyte infiltration were observed in ApoA-II$^{-/-}$ mice maintained under physiological conditions (Fig. 6*A*, 6*C*). However, once Con A was injected, ApoA-II$^{-/-}$ mice showed dramatically increased levels of AST and ALT as compared with those of WT mice (Fig. 6*A*). We also performed histological analysis of the liver. Without Con A injection, the livers of ApoA-II$^{-/-}$ mice showed slightly increased areas of glycogen accumulation (Fig. 6*B*, *bottom row*, *left*). After Con A injection, liver damage accompanied by increased numbers of apoptotic hepatocytes was apparently more severe in ApoA-II$^{-/-}$ mice as compared with that observed in WT mice (Fig. 6*B*, *right four panels*). Moreover, leukocyte infiltration into the liver 4 h after Con A injection was significantly higher in ApoA-II$^{-/-}$ mice (Fig.

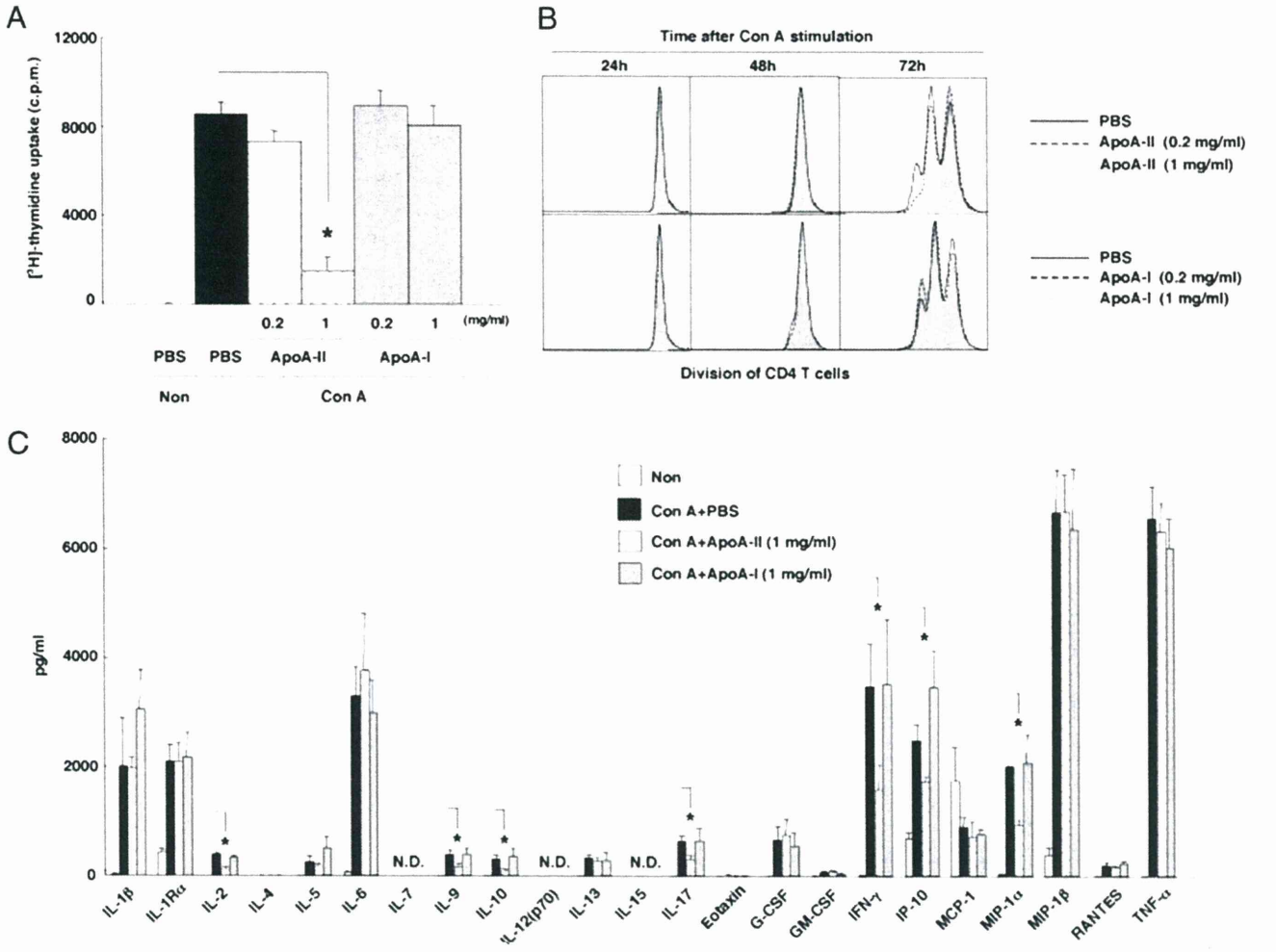

FIGURE 5. Suppression of the activation of human CD4 T cells. *A*, The proliferative response of human CD4 T cells was measured by [^{3}H]thymidine uptake. Purified human CD4 T cells were stimulated with Con A (5 μg/ml) for 40 h in the presence of ApoA-II or ApoA-I (0.2 or 1 mg/ml). The results are expressed as mean ± SD (n = 5). *$p < 0.05$, compared with PBS-added CD4 T cells. *B*, Purified human CD4 T cells were labeled with CFSE and stimulated with Con A in the presence of ApoA-II or ApoA-I. The division of CD4 T cells was assessed by flow cytometry. *C*, Purified human CD4 T cells were stimulated with Con A for 24 h in the presence of ApoA-II or ApoA-I, and the amounts of 23 cytokines in the culture supernatant were assessed by Bio-Plex. The results are expressed as mean ± SD (n = 5). *$p < 0.05$, compared with PBS-added CD4 T cells. Similar data were obtained from three independent experiments. N.D., not detected.

6*C*), and the increase in number of CD4 T cells in the liver of ApoA-II$^{-/-}$ mice was greater than that of WT mice (Fig. 6*D*). There was no significant difference in infiltration of macrophages or neutrophils into the liver 12 h after Con A injection between ApoA-II$^{-/-}$ and WT mice (Supplemental Fig. 2). The levels of IFN-γ production by Con A-stimulated ApoA-II$^{-/-}$ CD4 T cells were significantly higher than those in WT CD4 T cells, and the production of IFN-γ was equivalently inhibited by the addition of ApoA-II in WT and ApoA-II$^{-/-}$ groups (Fig. 6*E*). No significant difference in the production of IL-2 or the proliferation of CD4 T cells was detected between ApoA-II$^{-/-}$ and WT mice, whereas similar inhibition by ApoA-II was observed in CD4 T cells prepared from WT and ApoA-II$^{-/-}$ mice (Supplemental Fig. 3). Next, to confirm the critical role of IFN-γ– or IL-17–producing CD4 T cells in vivo in contributing to the liver injury in ApoA-II$^{-/-}$ mice during Con A-induced hepatitis, we depleted CD4 T cells, neutralized IFN-γ or IL-17 in ApoA-II$^{-/-}$ mice by the administration of anti-CD4, anti–IFN-γ, or anti–IL-17 mAb, and assessed the liver damage in response to Con A injection. Con A-induced hepatitis was protected almost completely by the injection of either anti-CD4 or anti–IFN-γ mAb in both WT and ApoA-II$^{-/-}$ mice, although no obvious protection after Con A injection was mediated by the injection of anti–IL-17 mAb (Fig. 6*F*). These results indicate that IFN-γ–producing CD4 T cells play an important role in the development and progression of Con A-induced hepatitis in both WT and ApoA-II$^{-/-}$ mice.

Attenuation of Con A-induced hepatitis by postadministration of ApoA-II

Finally, we assessed whether ApoA-II inhibits Con A-induced hepatitis even after the onset of hepatitis. We administered ApoA-II 2 h after injection of Con A, because approximately one and a half times the number of CD4 T cells was observed in the liver by this time (data not shown), and compared the efficacy of ApoA-II and a clinically used dose of prednisolone (4 mg/kg, i.v.) that is a standard treatment for autoimmune hepatitis patients. Preadministration of ApoA-II or prednisolone significantly suppressed the Con A-induced increase in the levels of AST and ALT, and the efficacy of prednisolone given before Con A injection was more potent than ApoA-II. Interestingly, postadministration of ApoA-II but not prednisolone significantly suppressed the Con A-induced increase in the levels of AST and ALT (Fig. 7*A*). We also observed no improvements using a higher dose (20 mg/kg, i.v.) of postadministration of prednisolone (data not shown). In addition,

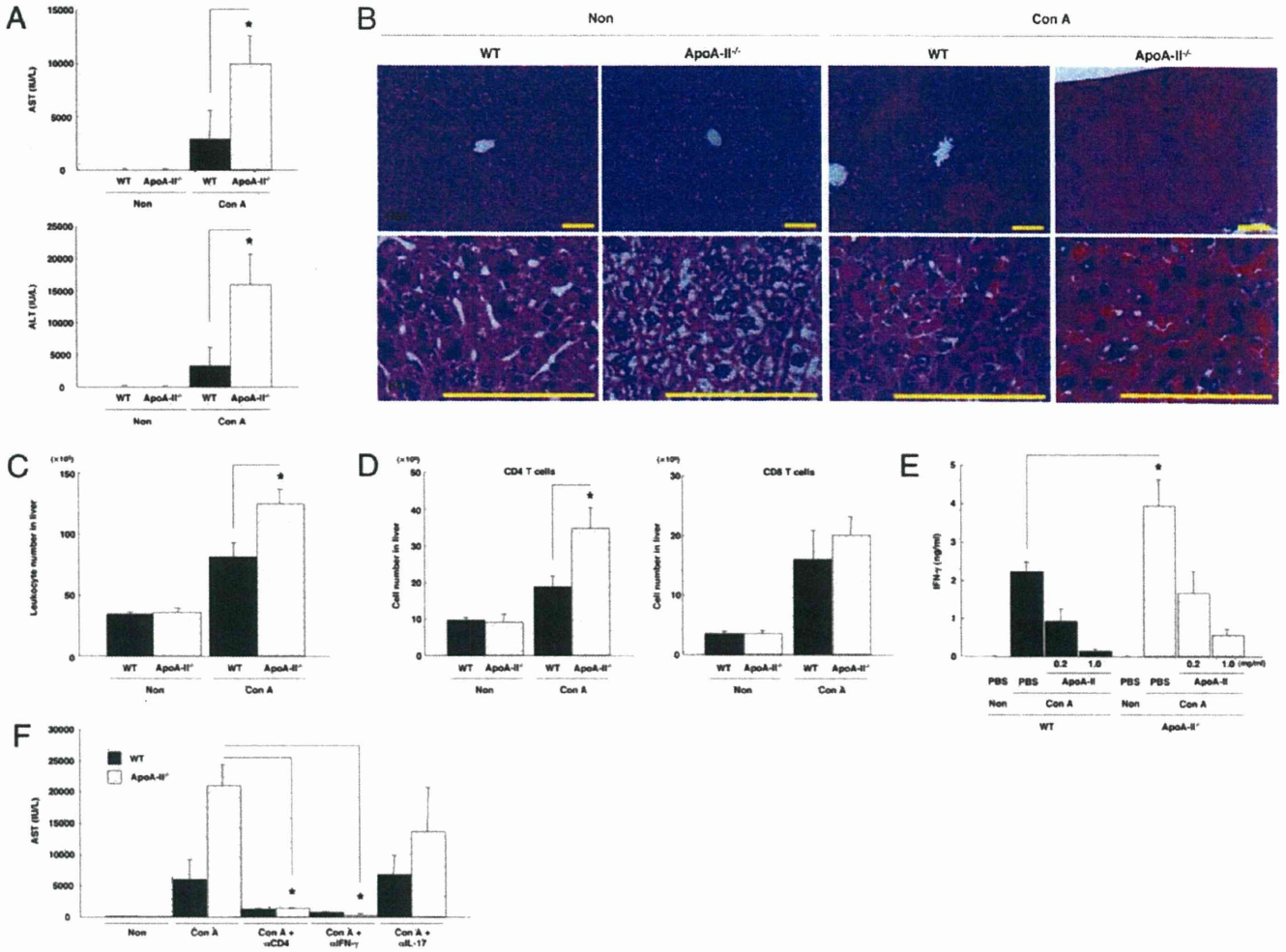

FIGURE 6. Exacerbation of Con A-induced hepatitis in ApoA-II$^{-/-}$ mice. *A*, Plasma AST and ALT levels in ApoA-II$^{-/-}$ and WT mice 12 h after Con A (20 mg/kg, i.v.) injection. The results are expressed as mean ± SD ($n = 7$). *$p < 0.05$, compared with WT mice. *B*, The livers were collected 12 h after Con A injection, and liver damage was evaluated by H&E staining. Scale bars, 100 μm (*upper* and *lower panels*). *C*, Total leukocyte cell numbers in the liver 4 h after the Con A injection into ApoA-II$^{-/-}$ or WT mice. The results are expressed as mean ± SD ($n = 6$). *$p < 0.05$, compared with WT mice. *D*, Flow cytometric analysis of liver mononuclear cells 4 h after Con A injection. The results are expressed as mean ± SD ($n = 6$). *$p < 0.05$, compared with WT mice. *E*, Purified splenic CD4 T cells from ApoA-II$^{-/-}$ and WT mice were stimulated with Con A (5 μg/ml) for 24 h in the presence of ApoA-II, and the amount of IFN-γ in the culture supernatant was assessed by ELISA. The results are expressed as mean ± SD ($n = 5$). *$p < 0.05$, compared with PBS-added CD4 T cells from WT mice. Similar data were obtained from three independent experiments. *F*, Plasma AST levels in ApoA-II$^{-/-}$ and WT mice 12 h after Con A injection. Anti-CD4 mAb was i.p. injected into ApoA-II$^{-/-}$ and WT mice 5, 3, and 1 d before Con A injection. Anti–IFN-γ mAb was i.v. injected into ApoA-II$^{-/-}$ and WT mice 30 min before Con A injection. Anti–IL-17 mAb was i.p. injected into ApoA-II$^{-/-}$ and WT mice 30 min before Con A injection. The results are expressed as mean ± SD ($n = 3$). *$p < 0.05$, compared with ApoA-II$^{-/-}$ mice.

Con A-induced histological damage such as severe necrosis and apoptosis of hepatocytes in the liver was also suppressed by postadministration of ApoA-II but not of prednisolone (Fig. 7*B*). The increased infiltration of leukocytes (Fig. 7*C*) and CD4 and CD8 T cells (Fig. 7*D*) into the liver was significantly suppressed by the postadministration of ApoA-II but not prednisolone (Fig. 7*C*, 7*D*). These results indicate that Con A-induced hepatitis is inhibited by ApoA-II administration even after the onset of hepatitis.

Discussion

In this report, we demonstrate clear evidence indicating that ApoA-II, which is the second major HDL in human plasma, has a suppressive effect on Con A-induced hepatitis. Exacerbated hepatitis was observed in ApoA-II$^{-/-}$ mice, indicating a physiological role for ApoA-II in the protection of Con A-induced hepatitis. The suppressive effect of ApoA-II was observed even after the onset of Con A-induced hepatitis. ApoA-II showed a potent suppressive effect on both mouse and human CD4 T cells. Therefore, ApoA-II could be used as a new relatively safe therapeutic agent for CD4 T cell-dependent autoimmune or viral hepatitis in humans.

Activated T cells and subsequent production of cytokines play a critical role in the pathogenesis of hepatitis. Upregulation of proinflammatory cytokines such as IFN-γ and TNF-α by Con A injection directly induce hepatocellular apoptosis and necrosis (13, 15, 35), with relatively more critical roles for IFN-γ having been suggested (36, 37). Although significantly decreased expression of both IFN-γ and TNF-α in the liver was detected (Fig. 2*C*), the in vitro experiments revealed that ApoA-II suppressed the production of IFN-γ but not TNF-α in Con A-stimulated mouse and human CD4 T cells (Figs. 4*C*, 5*C*). Activated CD8 T cells, which produce a high amount of IFN-γ, also contribute to the development of Con A-induced hepatitis, however less so as compared with CD4 T cells (12). ApoA-II also inhibited the production of IFN-γ in Con A-activated CD8 T cells (Supplemental Fig. 4). It is also known that macrophages and neutrophils are involved in the induction of Con A-induced hepatitis (38, 39),

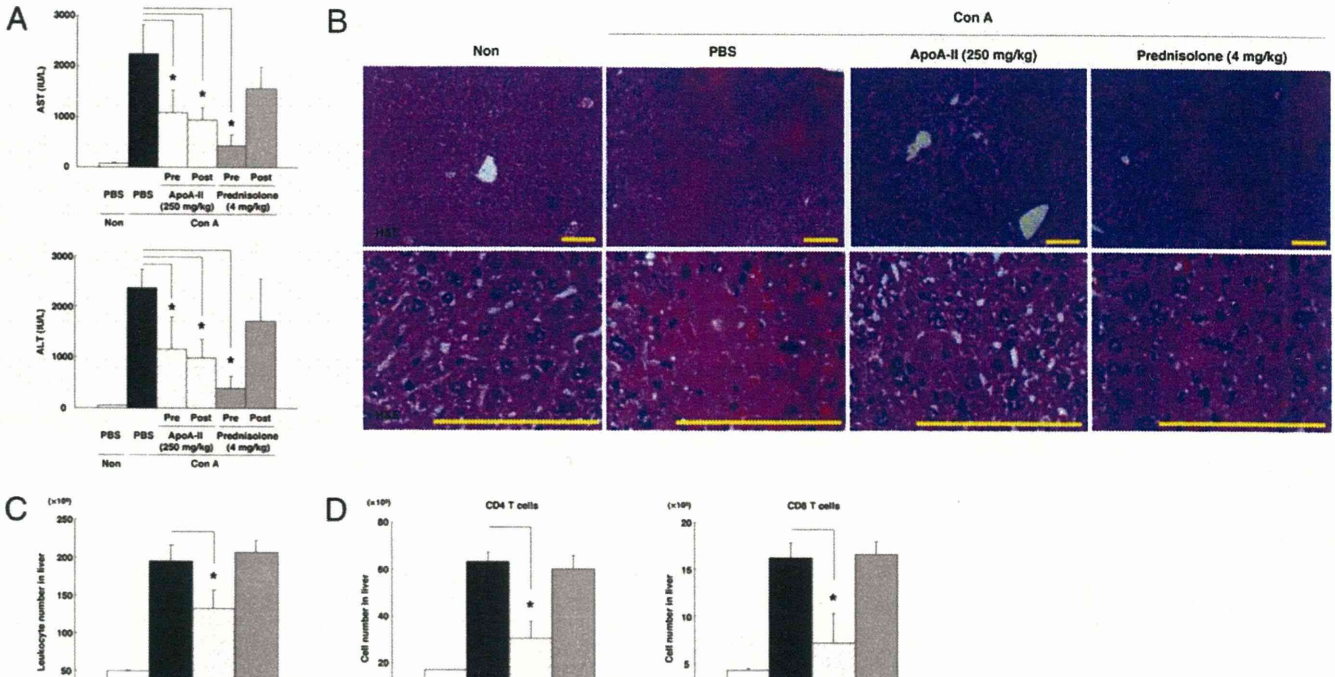

FIGURE 7. Attenuation of Con A-induced hepatitis by ApoA-II administration after the onset of hepatitis. *A*, Plasma AST and ALT levels in Con A-induced hepatitis in mice. Con A (12.5 mg/kg, i.v.) and PBS, Con A and ApoA-II (250 mg/kg, i.v.), or Con A and prednisolone (4 mg/kg, i.v.) were injected into BALB/c mice. Plasma was collected 12 h after Con A injection (pretreatment, 10 min before the injection of Con A; posttreatment, 2 h after the injection of Con A). The results are expressed as mean ± SD ($n = 6$). *$p < 0.05$, compared with PBS-administered mice. *B*, The livers were collected 12 h after the posttreatment of ApoA-II and prednisolone, and liver damage was evaluated by H&E staining. Scale bars, 100 μm (*upper* and *lower panels*). *C*, Total leukocyte cell numbers in the liver after Con A injection. Livers were collected 12 h after Con A injection. The results are expressed as mean ± SD ($n = 6$). *$p < 0.05$, compared with PBS-administered mice. *D*, Flow cytometric analysis of leukocyte infiltration into the liver 12 h after Con A injection. The numbers of CD4 or CD8 T cells are expressed as mean ± SD ($n = 6$). *$p < 0.05$, compared with PBS-administered mice.

because these cells can produce various cytokines and chemokines, leading to liver injury. However, the production of TNF-α from IFN-γ–stimulated peritoneal macrophages was not changed by ApoA-II (Supplemental Fig. 5*A*). ApoA-II also did not suppress TNF-α–induced activation of peritoneal neutrophils (Supplemental Fig. 5*B*), which was evaluated by the expression of activation markers for neutrophils, such as CD62L and CD11b (40). Previously, it was reported that IL-17–producing CD4 T cells also contributed to the induction of Con A-induced hepatitis (41). ApoA-II was capable of suppressing IL-17 production in activated CD4 T cells (Supplemental Fig. 6). However, no obvious protection in both WT and ApoA-II$^{-/-}$ mice after Con A injection was observed by the injection of anti–IL-17 mAb (Fig. 6*F*). In addition, ApoA-II injection did not alter the number of Foxp3$^+$ regulatory T cells (Tregs) among CD4 T cells infiltrating in the liver even after Con A injection, and also the number of Foxp3$^+$ Tregs was not reduced in the ApoA-II$^{-/-}$ mice (J. Yamashita, K. Kaneko, and T. Nakayama, unpublished observations). Thus, Th17 cells and Tregs may not play a major role in the attenuation of Con A-induced hepatitis by ApoA-II. Taken together, ApoA-II appears to attenuate Con A-induced hepatitis largely by the suppression of IFN-γ production by CD4 T cells.

The administration of ApoA-II suppressed the migration of CD4 T cells, CD8 T cells, macrophages, and neutrophils into the liver after Con A injection (Fig. 3*B*, 3*C*). We measured the expression of several chemoattractant factors and found that ApoA-II significantly suppressed the mRNA expression of MIP-1α, MIP-1β, and RANTES that attract CD4 T cells, CD8 T cells, and macrophages in the liver after Con A injection (Fig. 2*C*). Indeed, the increased production of MIP-1α, MIP-1β, and RANTES was reported in chronic hepatitis C (42–44), alcoholic hepatitis and cirrhosis (45), and transplanted liver (46, 47) in humans. In the mouse model, these chemokines also have an important role in the induction of hepatitis (33, 34). The infiltration of CD4 or CD8 T cells into the liver after Con A injection was more rapid as compared with that of macrophages and neutrophils (Fig. 3*C*). Therefore, the suppression of chemokine production from CD4 T cells by ApoA-II at the early stage of hepatitis could reduce the migration of macrophages and neutrophils, both of which are known to be involved in the pathogenesis of Con A-induced hepatitis. Previously, we and others reported that Vα14iNKT cells are rapidly activated, produce large amounts of IFN-γ after the injection of Con A, and can contribute to the development of Con A-induced hepatitis (16, 48, 49). Although we observed a decrease in the number of Vα14iNKT cells in the liver after Con A injection, the levels were equivalent between ApoA-II– and PBS-treated groups (Supplemental Fig. 7*A*). In addition, no obvious difference in the number of IFN-γ–producing Vα14iNKT cells in the spleen between ApoA-II– and PBS-treated mice was observed (Supplemental Fig. 7*B*). Thus, Vα14iNKT cells may not be involved in the process of inhibition of hepatitis by ApoA-II.

The activation of nuclear transcription factors such as AP-1, NFAT, and NF-κB are essential for the activation of T cells and the transcriptional upregulation of the various cytokine genes (50–53). ApoA-II inhibited the phosphorylation of ERK1/2 and c-Jun, a member of the AP-1 transcription factor family, and suppressed the nuclear translocation of NFATc1 in Con A-stimulated CD4 T cells (Fig. 4*D*, 4*E*). Thus, this could be the mechanism by which

ApoA-II inhibited the activation and IFN-γ production in CD4 T cells. In fact, cyclosporine A and FK506 (Tacrolimus) inhibited Con A-induced hepatitis through the inhibition of the activation of calcineurin, the upstream signaling molecule of NFAT activation and nuclear translocation (12).

We demonstrate a physiological role for ApoA-II in the protection from Con A-induced hepatitis using ApoA-II$^{-/-}$ mice (Fig. 6). CD4 T cells may play a more important role in this protection as compared with CD8 T cells, because selectively increased infiltration of CD4 T cells and their enhanced IFN-γ production were observed in ApoA-II$^{-/-}$ mice (Fig. 6*D*, 6*E*). In the liver of ApoA-II$^{-/-}$ mice, increased areas of glycogen accumulation were observed (Fig. 6*B*). Thus, the changes in lipoprotein metabolism in ApoA-II$^{-/-}$ mice could induce the malfunction of CD4 T cells leading to enhanced Con A-induced hepatitis. However, the upregulated CD4 T cell function, such as enhanced IFN-γ production, observed in ApoA-II$^{-/-}$ CD4 T cells was normalized by the addition of ApoA-II (Fig. 6*E*). Con A-induced production of IL-2 and proliferation were not significantly altered in ApoA-II$^{-/-}$ CD4 T cells and were equivalently inhibited by ApoA-II (Supplemental Fig. 3). Therefore, the basic function of CD4 T cells developed in ApoA-II$^{-/-}$ mice appeared to be normal. In any event, CD4 T cells appear to be the major target cells for the inhibitory effect of ApoA-II in Con A-induced hepatitis under physiological conditions.

Patients with autoimmune hepatitis usually require immunosuppressive therapy for many years. The immunosuppressive drugs, primarily glucocorticoids, serve as the standard therapy for autoimmune hepatitis (3, 4, 54, 55). Therefore, we compared the ability of ApoA-II and prednisolone to suppress Con A-induced hepatitis. Interestingly, postadministration of ApoA-II attenuated Con A-induced hepatitis, whereas the effect of prednisolone was less impressive (Fig. 7*A*, 7*B*). The postadministration of ApoA-II but not of prednisolone reduced leukocyte infiltration including CD4 and CD8 T cells into the liver (Fig. 7*C*, 7*D*). Thus, the mechanisms underlying the inhibition of Con A-induced hepatitis appeared to be distinct between ApoA-II and prednisolone. Because ApoA-II is a component of normal human plasma, side effects induced by the administration of ApoA-II could be marginal. In fact, preliminary preclinical experiments suggest that only marginal side effects are observed (J. Yamashita, K. Kaneko, and T. Nakayama, unpublished observations). Therefore, a combination therapy of ApoA-II with a low dose glucocorticoids and/or other immunosuppressive agents may prevent the severe side effects and consequently may prove that ApoA-II is an effective therapeutic agent for autoimmune hepatitis.

In summary, we showed that ApoA-II protected mice from Con A-induced hepatitis by suppressing the function of activated CD4 T cells and reducing the intrahepatic infiltration of inflammatory cells. Although we used ApoA-II prepared from human plasma in this study, we recently found that rApoA-II also attenuated Con A-induced hepatitis (J. Yamashita, K. Kaneko, and T. Nakayama, unpublished observations). Hence, our study offers new perspectives for the treatment of CD4 T cell-related autoimmune or viral hepatitis with ApoA-II in humans.

Acknowledgments

We thank Dr. Damon Tumes for helpful comments and constructive criticisms in the preparation of the manuscript. We thank Kaoru Sugaya, Hikari K. Asou, Satoko S. Norikane, and Toshihiro Ito for excellent technical assistance.

Disclosures

The authors have no financial conflicts of interest.

References

1. Alvarez, F., P. A. Berg, F. B. Bianchi, L. Bianchi, A. K. Burroughs, E. L. Cancado, R. W. Chapman, W. G. Cooksley, A. J. Czaja, V. J. Desmet, et al. 1999. International Autoimmune Hepatitis Group Report: review of criteria for diagnosis of autoimmune hepatitis. *J. Hepatol.* 31: 929–938.
2. Gregorio, G. V., B. Portmann, F. Reid, P. T. Donaldson, D. G. Doherty, M. McCartney, A. P. Mowat, D. Vergani, and G. Mieli-Vergani. 1997. Autoimmune hepatitis in childhood: a 20-year experience. *Hepatology* 25: 541–547.
3. Montano Loza, A. J., and A. J. Czaja. 2007. Current therapy for autoimmune hepatitis. *Nat. Clin. Pract. Gastroenterol. Hepatol.* 4: 202–214.
4. Heneghan, M. A., and I. G. McFarlane. 2002. Current and novel immunosuppressive therapy for autoimmune hepatitis. *Hepatology* 35: 7–13.
5. Bogdanos, D. P., G. Mieli-Vergani, and D. Vergani. 2000. Virus, liver and autoimmunity. *Dig. Liver Dis.* 32: 440–446.
6. Chang, K. M., R. Thimme, J. J. Melpolder, D. Oldach, J. Pemberton, J. Moorhead-Loudis, J. G. McHutchison, H. J. Alter, and F. V. Chisari. 2001. Differential CD4(+) and CD8(+) T-cell responsiveness in hepatitis C virus infection. *Hepatology* 33: 267–276.
7. Chedid, A., C. L. Mendenhall, T. E. Moritz, S. W. French, T. S. Chen, T. R. Morgan, G. A. Roselle, B. A. Nemchausky, C. H. Tamburro, E. R. Schiff, et al. 1993. Cell-mediated hepatic injury in alcoholic liver disease. Veterans Affairs Cooperative Study Group 275. *Gastroenterology* 105: 254–266.
8. Kita, H., I. R. Mackay, J. Van De Water, and M. E. Gershwin. 2001. The lymphoid liver: considerations on pathways to autoimmune injury. *Gastroenterology* 120: 1485–1501.
9. Rehermann, B., and F. V. Chisari. 2000. Cell mediated immune response to the hepatitis C virus. *Curr. Top. Microbiol. Immunol.* 242: 299–325.
10. Eggink, H. F., H. J. Houthoff, S. Huitema, C. H. Gips, and S. Poppema. 1982. Cellular and humoral immune reactions in chronic active liver disease. I. Lymphocyte subsets in liver biopsies of patients with untreated idiopathic autoimmune hepatitis, chronic active hepatitis B and primary biliary cirrhosis. *Clin. Exp. Immunol.* 50: 17–24.
11. Löhr, H. F., J. F. Schlaak, A. W. Lohse, W. O. Böcher, M. Arenz, G. Gerken, and K. H. Meyer Zum Büschenfelde. 1996. Autoreactive CD4+ LKM-specific and anticlonotypic T-cell responses in LKM-1 antibody-positive autoimmune hepatitis. *Hepatology* 24: 1416–1421.
12. Tiegs, G., J. Hentschel, and A. Wendel. 1992. A T cell-dependent experimental liver injury in mice inducible by concanavalin A. *J. Clin. Invest.* 90: 196–203.
13. Küsters, S., F. Gantner, G. Künstle, and G. Tiegs. 1996. Interferon gamma plays a critical role in T cell-dependent liver injury in mice initiated by concanavalin A. *Gastroenterology* 111: 462–471.
14. Mizuhara, H., M. Uno, N. Seki, M. Yamashita, M. Yamaoka, T. Ogawa, K. Kaneda, T. Fujii, H. Senoh, and H. Fujiwara. 1996. Critical involvement of interferon gamma in the pathogenesis of T-cell activation-associated hepatitis and regulatory mechanisms of interleukin-6 for the manifestations of hepatitis. *Hepatology* 23: 1608–1615.
15. Toyonaga, T., O. Hino, S. Sugai, S. Wakasugi, K. Abe, M. Shichiri, and K. Yamamura. 1994. Chronic active hepatitis in transgenic mice expressing interferon-gamma in the liver. *Proc. Natl. Acad. Sci. USA* 91: 614–618.
16. Kaneko, Y., M. Harada, T. Kawano, M. Yamashita, Y. Shibata, F. Gejyo, T. Nakayama, and M. Taniguchi. 2000. Augmentation of Valpha14 NKT cell-mediated cytotoxicity by interleukin 4 in an autocrine mechanism resulting in the development of concanavalin A-induced hepatitis. *J. Exp. Med.* 191: 105–114.
17. Miller, N. E. 1987. Associations of high-density lipoprotein subclasses and apolipoproteins with ischemic heart disease and coronary atherosclerosis. *Am. Heart J.* 113: 589–597.
18. Tall, A. R. 1990. Plasma high density lipoproteins. Metabolism and relationship to atherogenesis. *J. Clin. Invest.* 86: 379–384.
19. Bu, X., C. H. Warden, Y. R. Xia, C. De Meester, D. L. Puppione, S. Teruya, B. Lokensgard, S. Daneshmand, J. Brown, R. J. Gray, et al. 1994. Linkage analysis of the genetic determinants of high density lipoprotein concentrations and composition: evidence for involvement of the apolipoprotein A-II and cholesteryl ester transfer protein loci. *Hum. Genet.* 93: 639–648.
20. Vu-Dac, N., K. Schoonjans, V. Kosykh, J. Dallongeville, R. A. Heyman, B. Staels, and J. Auwerx. 1996. Retinoids increase human apolipoprotein A-II expression through activation of the retinoid X receptor but not the retinoic acid receptor. *Mol. Cell. Biol.* 16: 3350–3360.
21. Castellani, L. W., M. Navab, B. J. Van Lenten, C. C. Hedrick, S. Y. Hama, A. M. Goto, A. M. Fogelman, and A. J. Lusis. 1997. Overexpression of apolipoprotein AII in transgenic mice converts high density lipoproteins to proinflammatory particles. *J. Clin. Invest.* 100: 464–474.
22. Alexander, E. T., M. Tanaka, M. Kono, H. Saito, D. J. Rader, and M. C. Phillips. 2009. Structural and functional consequences of the Milano mutation (R173C) in human apolipoprotein A-I. *J. Lipid Res.* 50: 1409–1419.
23. Weng, W., and J. L. Breslow. 1996. Dramatically decreased high density lipoprotein cholesterol, increased remnant clearance, and insulin hypersensitivity in apolipoprotein A-II knockout mice suggest a complex role for apolipoprotein A-II in atherosclerosis susceptibility. *Proc. Natl. Acad. Sci. USA* 93: 14788–14794.
24. Weng, W., N. A. Brandenburg, S. Zhong, J. Halkias, L. Wu, X. C. Jiang, A. Tall, and J. L. Breslow. 1999. ApoA-II maintains HDL levels in part by inhibition of hepatic lipase. Studies In apoA-II and hepatic lipase double knockout mice. *J. Lipid Res.* 40: 1064–1070.
25. Cohn, E. J., J. L. Oncley, L. E. Strong, W. L. Hughes, and S. H. Armstrong. 1944. Chemical, clinical, and immunological studies on the products of human plasma fractionation. I. The characterization of the protein fractions of human plasma. *J. Clin. Invest.* 23: 417–432.

26. Peitsch, M. C., A. Kress, P. G. Lerch, J. J. Morgenthaler, H. Isliker, and H. J. Heiniger. 1989. A purification method for apolipoprotein A-I and A-II. *Anal. Biochem.* 178: 301–305.
27. Yang, K. S., S. W. Kang, H. A. Woo, S. C. Hwang, H. Z. Chae, K. Kim, and S. G. Rhee. 2002. Inactivation of human peroxiredoxin I during catalysis as the result of the oxidation of the catalytic site cysteine to cysteine-sulfinic acid. *J. Biol. Chem.* 277: 38029–38036.
28. Kimura, M. Y., H. Hosokawa, M. Yamashita, A. Hasegawa, C. Iwamura, H. Watarai, M. Taniguchi, T. Takagi, S. Ishii, and T. Nakayama. 2005. Regulation of T helper type 2 cell differentiation by murine Schnurri-2. *J. Exp. Med.* 201: 397–408.
29. Goossens, P. L., H. Jouin, G. Marchal, and G. Milon. 1990. Isolation and flow cytometric analysis of the free lymphomyeloid cells present in murine liver. *J. Immunol. Methods* 132: 137–144.
30. Watanabe, H., K. Ohtsuka, M. Kimura, Y. Ikarashi, K. Ohmori, A. Kusumi, T. Ohteki, S. Seki, and T. Abo. 1992. Details of an isolation method for hepatic lymphocytes in mice. *J. Immunol. Methods* 146: 145–154.
31. Kimura, M., Y. Koseki, M. Yamashita, N. Watanabe, C. Shimizu, T. Katsumoto, T. Kitamura, M. Taniguchi, H. Koseki, and T. Nakayama. 2001. Regulation of Th2 cell differentiation by mel-18, a mammalian polycomb group gene. *Immunity* 15: 275–287.
32. Yamashita, M., M. Kimura, M. Kubo, C. Shimizu, T. Tada, R. M. Perlmutter, and T. Nakayama. 1999. T cell antigen receptor-mediated activation of the Ras/mitogen-activated protein kinase pathway controls interleukin 4 receptor function and type-2 helper T cell differentiation. *Proc. Natl. Acad. Sci. USA* 96: 1024–1029.
33. Ajuebor, M. N., C. M. Hogaboam, T. Le, A. E. Proudfoot, and M. G. Swain. 2004. CCL3/MIP-1alpha is pro-inflammatory in murine T cell-mediated hepatitis by recruiting CCR1-expressing CD4(+) T cells to the liver. *Eur. J. Immunol.* 34: 2907–2918.
34. Leifeld, L., F. L. Dumoulin, I. Purr, K. Janberg, C. Trautwein, M. Wolff, M. P. Manns, T. Sauerbruch, and U. Spengler. 2003. Early up-regulation of chemokine expression in fulminant hepatic failure. *J. Pathol.* 199: 335–344.
35. Gantner, F., M. Leist, A. W. Lohse, P. G. Germann, and G. Tiegs. 1995. Concanavalin A-induced T-cell-mediated hepatic injury in mice: the role of tumor necrosis factor. *Hepatology* 21: 190–198.
36. Tagawa, Y., K. Sekikawa, and Y. Iwakura. 1997. Suppression of concanavalin A-induced hepatitis in IFN-gamma(-/-) mice, but not in TNF-alpha(-/-) mice: role for IFN-gamma in activating apoptosis of hepatocytes. *J. Immunol.* 159: 1418–1428.
37. Kano, A., T. Haruyama, T. Akaike, and Y. Watanabe. 1999. IRF-1 is an essential mediator in IFN-gamma-induced cell cycle arrest and apoptosis of primary cultured hepatocytes. *Biochem. Biophys. Res. Commun.* 257: 672–677.
38. Bonder, C. S., M. N. Ajuebor, L. D. Zbytnuik, P. Kubes, and M. G. Swain. 2004. Essential role for neutrophil recruitment to the liver in concanavalin A-induced hepatitis. *J. Immunol.* 172: 45–53.
39. Gantner, F., M. Leist, S. Küsters, K. Vogt, H. D. Volk, and G. Tiegs. 1996. T cell stimulus-induced crosstalk between lymphocytes and liver macrophages results in augmented cytokine release. *Exp. Cell Res.* 229: 137–146.
40. Bournazou, I., J. D. Pound, R. Duffin, S. Bournazos, L. A. Melville, S. B. Brown, A. G. Rossi, and C. D. Gregory. 2009. Apoptotic human cells inhibit migration of granulocytes via release of lactoferrin. *J. Clin. Invest.* 119: 20–32.
41. Nagata, T., L. McKinley, J. J. Peschon, J. F. Alcorn, S. J. Aujla, and J. K. Kolls. 2008. Requirement of IL-17RA in Con A induced hepatitis and negative regulation of IL-17 production in mouse T cells. *J. Immunol.* 181: 7473–7479.
42. Narumi, S., Y. Tominaga, M. Tamaru, S. Shimai, H. Okumura, K. Nishioji, Y. Itoh, and T. Okanoue. 1997. Expression of IFN-inducible protein-10 in chronic hepatitis. *J. Immunol.* 158: 5536–5544.
43. Shields, P. L., C. M. Morland, M. Salmon, S. Qin, S. G. Hubscher, and D. H. Adams. 1999. Chemokine and chemokine receptor interactions provide a mechanism for selective T cell recruitment to specific liver compartments within hepatitis C-infected liver. *J. Immunol.* 163: 6236–6243.
44. Kusano, F., Y. Tanaka, F. Marumo, and C. Sato. 2000. Expression of C-C chemokines is associated with portal and periportal inflammation in the liver of patients with chronic hepatitis C. *Lab. Invest.* 80: 415–422.
45. Afford, S. C., N. C. Fisher, D. A. Neil, J. Fear, P. Brun, S. G. Hubscher, and D. H. Adams. 1998. Distinct patterns of chemokine expression are associated with leukocyte recruitment in alcoholic hepatitis and alcoholic cirrhosis. *J. Pathol.* 186: 82–89.
46. Adams, D. H., S. Hubscher, J. Fear, J. Johnston, S. Shaw, and S. Afford. 1996. Hepatic expression of macrophage inflammatory protein-1 alpha and macrophage inflammatory protein-1 beta after liver transplantation. *Transplantation* 61: 817–825.
47. Schenk, M., A. Zipfel, C. Schulz, H. D. Becker, and R. Viebahn. 2000. RANTES in the postoperative course after liver transplantation. *Transpl. Int.* 13(Suppl. 1): S147–S149.
48. Ajuebor, M. N., A. I. Aspinall, F. Zhou, T. Le, Y. Yang, S. J. Urbanski, S. Sidobre, M. Kronenberg, C. M. Hogaboam, and M. G. Swain. 2005. Lack of chemokine receptor CCR5 promotes murine fulminant liver failure by preventing the apoptosis of activated CD1d-restricted NKT cells. *J. Immunol.* 174: 8027–8037.
49. Diao, H., S. Kon, K. Iwabuchi, C. Kimura, J. Morimoto, D. Ito, T. Segawa, M. Maeda, J. Hamuro, T. Nakayama, et al. 2004. Osteopontin as a mediator of NKT cell function in T cell-mediated liver diseases. *Immunity* 21: 539–550.
50. Rooney, J. W., T. Hoey, and L. H. Glimcher. 1995. Coordinate and cooperative roles for NF-AT and AP-1 in the regulation of the murine IL-4 gene. *Immunity* 2: 473–483.
51. Kopp, E. B., and S. Ghosh. 1995. NF-kappa B and rel proteins in innate immunity. *Adv. Immunol.* 58: 1–27.
52. Rao, A. 1994. NF-ATp: a transcription factor required for the co-ordinate induction of several cytokine genes. *Immunol. Today* 15: 274–281.
53. Rao, A., C. Luo, and P. G. Hogan. 1997. Transcription factors of the NFAT family: regulation and function. *Annu. Rev. Immunol.* 15: 707–747.
54. Czaja, A. J., and H. A. Carpenter. 2004. Decreased fibrosis during corticosteroid therapy of autoimmune hepatitis. *J. Hepatol.* 40: 646–652.
55. Jones, E. A., and N. V. Bergasa. 1993. Immunosuppressive treatment of chronic liver disease. *Ann. N. Y. Acad. Sci.* 696: 319–327.

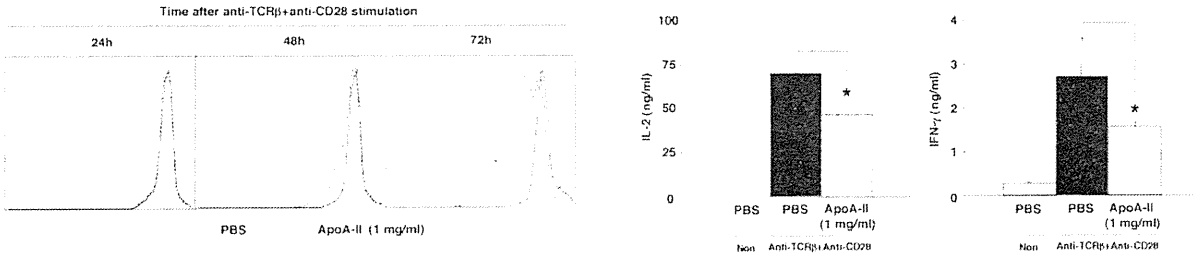

Supplemental Figure 1. ApoA-II suppresses the function of mouse CD4 T cells stimulated with anti-TCRβ plus anti-CD28. Purified mouse splenic CD4 T cells were labeled with CFSE and stimulated with immobilized anti-TCRβ mAb plus anti-CD28 mAb in the presence of ApoA-II (1 mg/ml) for 24, 48 and 72 h, and the amounts of IL-2 and IFN-γ in the culture supernatants after 24 h stimulation were assessed by ELISA. The results are expressed as mean ± SD. *$P < 0.05$, compared with PBS-added CD4 T cells.

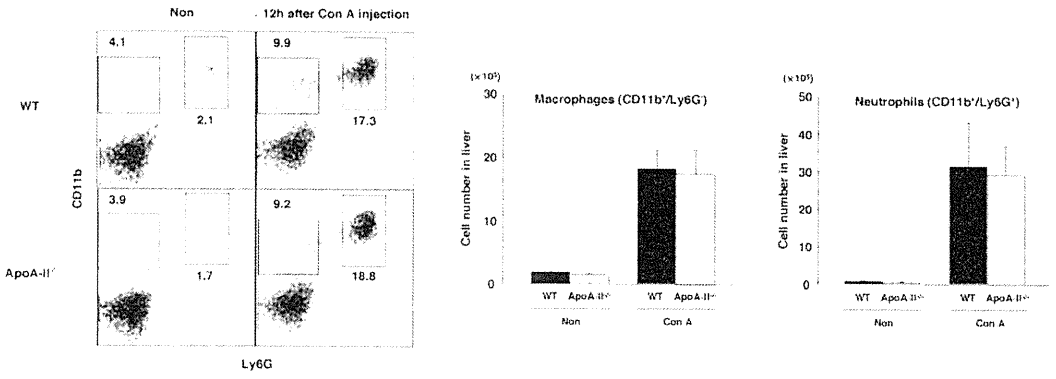

Supplemental Figure 2. Normal Con A-induced infiltration of macrophages and neutrophils into the liver in ApoA-II$^{-/-}$ mice. Con A (20 mg/kg, i.v.) was injected into ApoA-II$^{-/-}$ mice. Flow cytometric analysis was performed to assess the infiltration of macrophages and neutrophils into the liver 12 h after Con A injection. The numbers of CD11b^{+}/Ly6G^{-} cells and CD11b^{+}/Ly6G^{+} cells and were calculated using total leukocyte cell counts and flow cytometric analysis data. The results are expressed as mean ± SD (n=6).

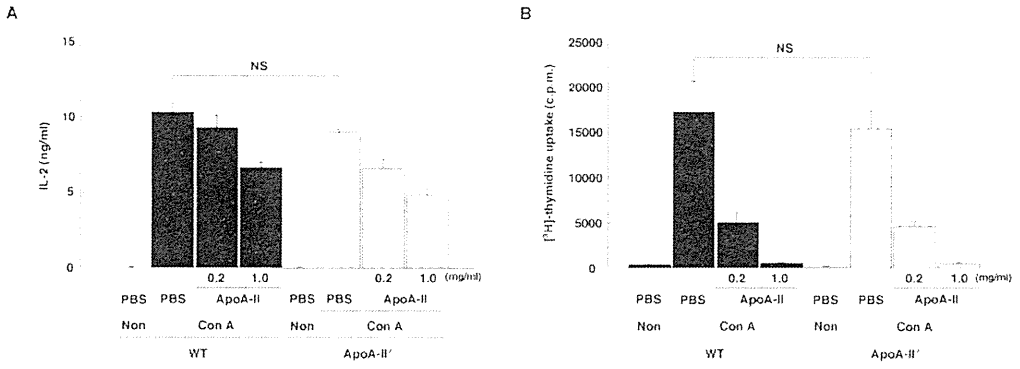

Supplemental Figure 3. The suppressive effect of ApoA-II is observed for both IL-2 production and proliferation in Con A-stimulated ApoA-II$^{-/-}$ CD4 T cells. (A), Purified splenic CD4 T cells from ApoA-II$^{-/-}$ and WT mice were stimulated with Con A (5 μg/ml) for 24 h in the presence of ApoA-II, and the amount of IL-2 in the culture supernatant was assessed by ELISA. The results are expressed as mean ± SD. **(B),** The proliferative response of splenic CD4 T cells was examined by [^{3}H]-thymidine uptake. Purified splenic CD4 T cells from ApoA-II$^{-/-}$ and WT mice were stimulated with Con A for 40 h in the presence of ApoA-II. The results are expressed as mean ± SD. Similar data were obtained from three independent experiments.

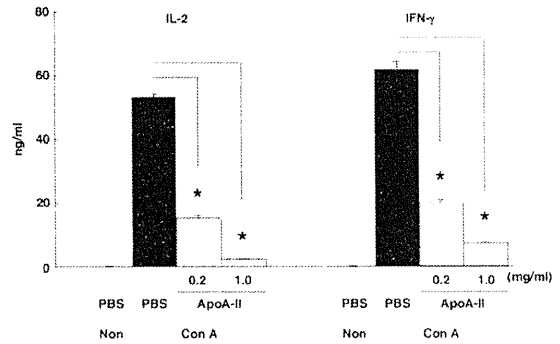

Supplemental Figure 4. Suppression of the function of mouse CD8 T cells by ApoA-II. Splenic CD8 T cells were purified from BALB/c splenocytes using PE-conjugated anti-CD8 mAb, anti-PE magnetic beads (Miltenyi Biotec), and Auto-MACS cell Sorter (Miltenyi Biotec). The purified CD8 T cells were stimulated with Con A (5 μg/ml) for 24 h in the presence of ApoA-II (0.2 or 1 mg/ml), and the amounts of IL-2 and IFN-γ in the culture supernatant were assessed by ELISA. The results are expressed as mean ± SD. *$P < 0.05$, compared with PBS-added CD8 T cells. Similar data were obtained from three independent experiments.

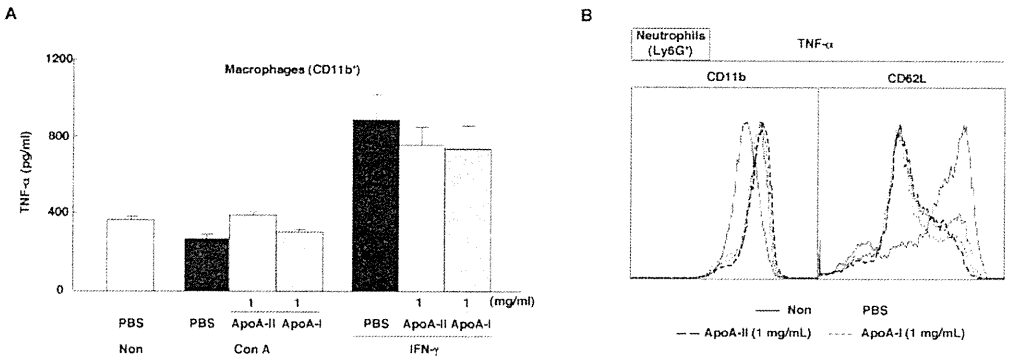

Supplemental Figure 5. ApoA-II does not suppress the function of macrophages or the activation of neutrophils. (A), To collect macrophages, 1 ml of 4% fluid thioglycollate medium (Sigma-Aldrich) was injected intraperitoneally into BALB/c mice. The peritoneal lavage cells were harvested on day 4 after the thioglycollate injection. Macrophages were purified using FITC-conjugated anti-CD11b mAb, anti-FITC magnetic beads, and Auto-MACS cell Sorting. Purified CD11b-positive cells consisted of more than 95% macrophages identified by flow cytometry and Wright-Giemsa staining, respectively (data not shown). Purified peritoneal macrophages were stimulated with Con A (5 μg/ml) or IFN-γ (2.5 ng/ml) for 24 h in the presence of ApoA-II or ApoA-I (1 mg/ml), and the amount of TNF-α in the culture supernatant was assessed by ELISA. The results are expressed as mean ± SD (n=5). **(B),** To collect neutrophils, 1 ml of 4% fluid thioglycollate medium was injected intraperitoneally into BALB/c mice. The peritoneal lavage cells were harvested 4 h after thioglycollate injection. Neutrophils were purified using PE-conjugated anti-Ly6G mAb, anti-PE magnetic beads, and Auto-MACS cell Sorting. The purified Ly6G-positive cells consisted of more than 95% neutrophils identified by flow cytometry and Wright-Giemsa staining (data not shown). Purified peritoneal neutrophils were stimulated with TNF-α (1 ng/ml) for 0.5 h in the presence of ApoA-II or ApoA-I, and the expression of CD11b and CD62L was assessed using flow cytometry.

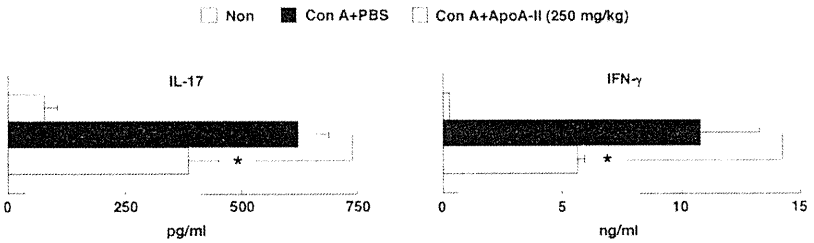

Supplemental Figure 6. The suppressive effect of ApoA-II administration on IL-17 production by mouse liver-infiltrating CD4 T cells after Con A injection. Con A (12.5 mg/kg, i.v.) and vehicle, or Con A and ApoA-II (250 mg/kg, i.v.) were administered into BALB/c mice. 12 h after Con A injection, liver CD4 T cells were purified from mice using FITC-conjugated anti-CD4 mAb, anti-FITC magnetic beads, and Auto-MACS cell Sorter. The purified CD4 T cells were stimulated with Con A (5 μg/ml) for 24 h, and the amounts of IFN-γ and IL-17 in the culture supernatant were assessed by ELISA. The results are expressed mean ± SD (n=4). *$P < 0.05$, compared with PBS-administrated mice.

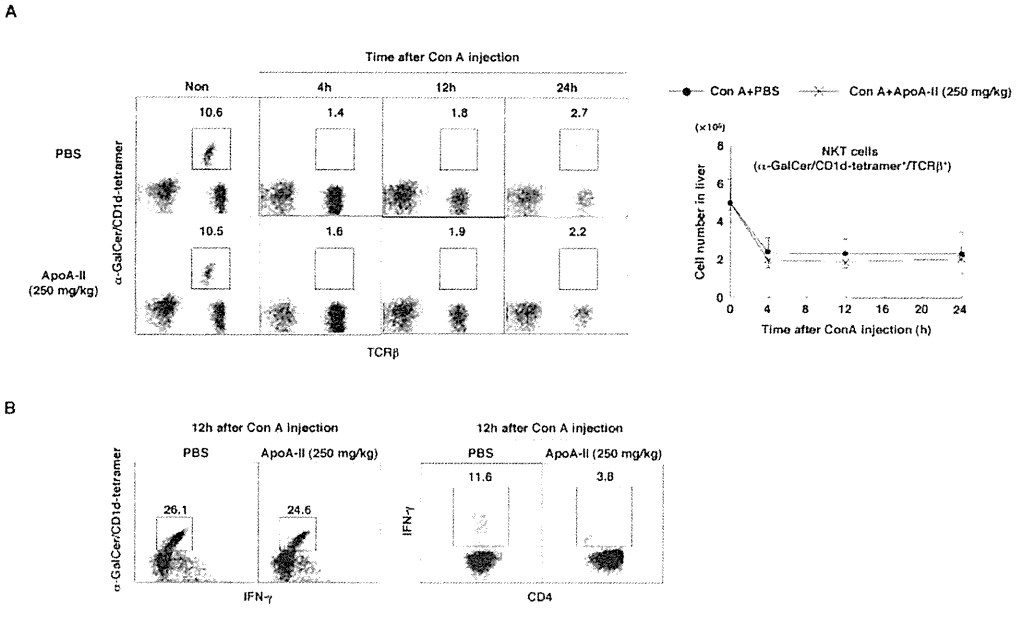

Supplemental Figure 7. ApoA-II administration did not change the activation of Vα14 NKT cell in the liver. **(A),** Con A (12.5 mg/kg, i.v.) and vehicle, or Con A and ApoA-II (250 mg/kg, i.v.) were administered into BALB/c mice. Flow cytometric analysis of Vα14 NKT cells in the liver 4, 12, and 24 h after Con A injection was performed to determine the expression profiles of α-GalCer/CD1d-tetramer$^+$ and TCRβ$^-$ cells. The number of α-GalCer/CD1d-tetramer$^+$/TCRβ$^+$ cells was calculated based on the total leukocyte cell counts and flow cytometric analysis data. The results are expressed as mean ± SD (n=8). **(B),** The intracellular expression of IFN-γ in α-GalCer/CD1d-tetramer$^+$ NKT cells or CD4 T cells in spleen 12h after Con A injection were analyzed using a Cytofix/Cytoperm Kit Plus (with Golgistop; BD Biosciences) according to the manufacturer's instructions.

Clinical Immunology (2011) 139, 267–276

available at www.sciencedirect.com

Clinical Immunology

www.elsevier.com/locate/yclim

Repressor of GATA negatively regulates murine contact hypersensitivity through the inhibition of type-2 allergic responses

Yoshiro Hirasaki[a,b], Chiaki Iwamura[a], Masakatsu Yamashita[a], Toshihiro Ito[a], Masayuki Kitajima[a], Kenta Shinoda[a], Takao Namiki[b], Katsutoshi Terasawa[b], Toshinori Nakayama[a,*]

[a] *Department of Immunology, Graduate School of Medicine, Chiba University, 1-8-1 Inohana, Chuo-ku, Chiba 260–8670, Japan*

[b] *Department of Japanese-Oriental Medicine, Graduate School of Medicine, Chiba University, 1-8-1 Inohana, Chuo-ku, Chiba 260–8670, Japan*

Received 4 November 2010; accepted with revision 1 February 2011
Available online 12 March 2011

KEYWORDS
Contact hypersensitivity;
Repressor of GATA (ROG);
Th2 responses;
Mast cell degranulation

Abstract Repressor of GATA (ROG) inhibits Th2 cell differentiation and allergic airway inflammation in the lung. To determine the role of ROG in the pathogenesis of contact hypersensitivity (CHS), a hapten-induced mouse model of CHS using ROG Tg and ROG-deficient ($ROG^{-/-}$) was used. ROG Tg mice showed little ear swelling, while $ROG^{-/-}$ mice showed enhanced ear swelling in comparison to wild type mice. Interstitial edema and mast cell degranulation at the local inflammation sites were mild in ROG Tg mice and exacerbated in $ROG^{-/-}$ mice. In addition, the serum total IgE and hapten-specific IgG1 levels were increased in $ROG^{-/-}$ mice. Adoptive transfer of $ROG^{-/-}$ $CD4^+$ T cells exacerbated CHS in wild type mice, while transfer of ROG Tg $CD4^+$ T cells resulted in the attenuation of CHS. These results indicate ROG negatively regulates the induction of CHS by controlling the $CD4^+$ T cell-mediated allergic responses, including IgE generation and mast cell degranulation.

1. Introduction

Contact dermatitis in humans is often caused by chemicals such as fragrance, nickel sulfate, cobalt chloride and numerous other agents. It is the most common occupational skin disease (OSD) in Western countries, and represents approximately 90–95% of all OSD. It also has a profound effect on workplace productivity [1–4]. Allergic contact

Abbreviations: CHS, Contact hypersensitivity; DNBS, Dinitrobenzene sulfonic acid; DNFB, 2,4-dinitrofluorobenzene; DNP, Dinitrophenol; ROG, Repressor of GATA; ROG-deficient, $ROG^{-/-}$; OSD, Occupational skin disease; AD, Atopic dermatitis.

* Corresponding author. Fax: +81 43 227 1498.
E-mail address: tnakayama@faculty.chiba-u.jp (T. Nakayama).

1521-6616/$ – see front matter © 2011 Elsevier Inc. All rights reserved.
doi:10.1016/j.clim.2011.02.009

hypersensitivity (CHS) typically shows delayed type hypersensitivity, which is mediated mainly by cellular factors. The effector phase of CHS is mediated mainly by $CD8^+$ T cells, whose functions are supported by Th1 cells [5]. $CD8^+$ T cells induce apoptosis of the epidermis of the skin followed by proinflammatory cellular infiltration [5–11]. On the other hand, there have been a few reports indicating that mast cells, IgE and Th2 cells play an important role in CHS [12–18].

Naïve $CD4^+$ T cells differentiate into several functionally-distinct subsets upon antigen recognition by TCR. Several distinct CD4 T cell subsets, including Th1, Th2, Th17, iTreg and Th9 cells have been identified based on their cytokine production properties, and Th2 cells are involved in allergic reactions [19]. Upon activation, Th2 cells secrete IL-4, IL-5 and IL-13 and provide help to B cells to produce IgE and IgG1, which ultimately lead to the occurrence of allergy. The zinc finger transcription factor GATA3 is the master regulator of Th2 cell differentiation. Besides being a transcription factor for the IL-5 and IL-13 genes, GATA3 regulates Th2 differentiation by inducing chromatin remodeling of the Th2 cytokine locus [20–24]. In addition, GATA3 is one of the most important allergy susceptibility genes in humans as identified by genome-wide association studies [25].

ROG, repressor of GATA, is a POZ (BTB) domain-containing Kruppel type zinc finger family (or POK family) repressor, and is highly homologous to other POK family proteins, such as BCL6 (B-cell lymphoma 6) and PLZF (promyelocytic leukemia zinc finger) [26,27]. A critical role of BCL6 for the generation of follicular helper T cells [28–30] and that of PLZF for NKT cell generation have been reported [31]. In addition, these proteins contain the Broad Complex, Tramtrack, and Bric á Brac/pox virus and zinc finger (BTB/POZ) domains in the N terminus, which mediates dimerization and recruits corepressor molecules to exert suppressive function[26,32]. In addition, the expression level of ROG in $CD8^+$ T cells is about ten times greater than that of $CD4^+$ Th2 cells [33]. Experiments in a mouse model of asthma demonstrated that the ROG plays an inhibitory role in allergic inflammation [34]. The present study used a hapten-induced mouse model of CHS and ROG-Tg and ROG-deficient mice, and found that ROG negatively regulates the induction of CHS by inhibiting the Th2 cell-mediated allergic responses.

2. Materials and methods

2.1. Mice

C57BL/6 mice were purchased from CLEA Japan (Tokyo). ROG transgenic (Tg) mice, under the control of the lck proximal promoter that confers a T-cell specific overexpression of the transgene and $ROG^{-/-}$ mice were generated in our laboratory as described in a previous report [34]. $ROG^{-/-}$ mice and ROG Tg mice were backcrossed to C57BL/6 more than 10 times. $ROG^{-/-}$ mice and ROG Tg mice were not crossed with OVA-specific TCRab Tg mice. A sex-matched 7–10 week-old group of 4 to 6 mice was used in the experiments. All mice used in this study were maintained under specific pathogen-free conditions. All animal care was conducted in accordance with the guidelines of Chiba University.

2.2. Contact hypersensitivity (CHS) assay

The mice were sensitized by shaving their ventral abdomen and applying 30 µl of 0.5% 2,4-dinitrofluorobenzene (DNFB; Sigma-Aldrich, USA) in 4:1 acetone/olive oil consecutively on days 0 and 1. Five days later, the mice were challenged with 20 µl of 0.5% DNFB on both sides of their left ear. Their right ears were treated with vehicle (the same amount of acetone/olive oil). Subsequently, the allergic dermatitis was assessed by measuring the thickness of the ears, using a micrometer (Quick-Mini Mitutoyo, Kanagawa Japan). The extent of ear swelling was scored as the differential thickness between the treated versus the control ear of the mice. The average thickness of each ear was determined by measuring three points of each ear.

2.3. Histology

The ear pinnae specimens were taken 48 h after challenge at the time of the maximum swelling. Then they were stained with hematoxylin–eosin or by May–Grunewald Giemsa stain for histological analyses. An immunohistochemical analysis was performed as described previously [35].

2.4. Evaluation of cytokine production from $CD8^+$ T cells

The regional lymph node cell suspension taken on day 8 was prepared after sensitization on days 1 and 2, and a challenge on day 6. Purified $CD8^+$ T cells (2×10^5) from each group were cultured in round bottom 96 well plates with 100 µg/ml DNBS and irradiated splenic APCs (1×10^6) for 72 h. Then, the supernatants were collected to measure cytokine concentrations by ELISA as described previously [34].

2.5. Hapten-specific CTL assay

A hapten-specific CTL assay was performed as previously described with some modifications [36]. In brief, cervical lymph nodes, recovered from DNFB-treated or non-treated mice on day 9 after being sensitized twice on their abdomen on days 1 and 2, and a challenge to the left ear on day 7, were tested for hapten-specific CTL activity. $CD8^+$ T cells were purified using magnetic beads and an auto-MACS Sorter™ (Miltenyi Biotec, Gladbach Germany). The $CD8^+$ T cells were restimulated with 3.8 ng/ml of IL-2 for 12 h *in vitro*. These cells were then assayed for cytolytic activity against EL-4 targets which had been cultured with 4 mM DNBS for 24 h. Target EL-4 cells (1×10^7) were chromium labeled by incubating them for 1 h at 37 °C with 1.3 Mbq ^{51}Cr (Chromium-51 Radionuclide, 37 Mbq/ml, PerkinElmer Life & Analytical Sciences). Varying degrees of diluted effector cells were plated in round-bottom microculture plates with ^{51}Cr-labeled EL-4 targets (1×10^4). The plates were then incubated at 37 °C for 4 h, and the radioactivity released in the supernatant was counted using a gamma counter. The results are expressed as the percent specific lysis ± SD calculated as follows: (cpm test − spontaneous cpm) / (maximal cpm − spontaneous cpm) × 100, where the maximal or spontaneous cpm represents the radioactivity released by targets exposed to 2% NP40 or medium, respectively.

2.6. Measurement of serum antibodies

Serum total IgE and dinitrophenol (DNP)-specific IgG1 were measured by ELISA as previously described [15]. In brief, 96-well plates (Nunc) were coated with DNP-OVA (50 μg/ml). After incubation with mouse serum for 1.5 h at 37 °C, DNP-specific IgG1 was detected with horseradish peroxidase-conjugated anti-mouse IgG1 (Zymed).

2.7. Adoptive transfer experiments

The adoptive transfer experiments were carried out by transferring DNFB-sensitized splenic $CD8^+$ T cells, $CD4^+$ T cells or the serum from the three groups of donor mice ($ROG^{+/+}$, ROG Tg, and $ROG^{-/-}$ mice), into 7-week-old wild type syngeneic C57BL/6 recipient mice. The mice in each group were sensitized to DNFB on days 0 and 1 as described above. The mice were sacrificed on day 6 and their splenic cells were prepared. $CD8^+$ T cells or $CD4^+$ T cells were negatively sorted using an auto-MACS Sorter using a $CD8^+$ T cell isolation kit or a $CD4^+$ T cell isolation kit (Milteny Biotec, Gladbach Germany), respectively according to the manufacturer's instructions. Then the $CD8^+$ T cells (3×10^6) or $CD4^+$ T cells (3×10^6) were transferred intravenously to the recipients. We treated recipient mice in two different ways. The recipient mice were first challenged on the following day of transfer, were sensitized once after transfer and then challenged. The ear thickness of the recipient mice was measured after the challenge. The serum transfer experiment was performed by sensitizing donor mice on days 0, 1 and 7. Then, 300 μl of serum from these mice was transferred into the recipients intraperitoneally on day 9, and the ear swelling responses were evaluated after challenge. Illustrations of the sensitization and challenge protocol are shown in the figures about the adoptive transfer experiments.

2.8. Statistical analysis

Statistical significance was evaluated with the unpaired two-tailed Student's *t*-test in all experiments. $p<0.05$ was considered to be significant.

3. Results

3.1. 2,4-dinitrofluorobenzene-induced ear swelling in ROG Tg and $ROG^{-/-}$ mice

First, we observed contact hypersensitivity induced by 2,4-dinitrofluorobenzene (DNFB) in wild type, ROG Tg, and $ROG^{-/-}$ mice, in which the cell number and the phenotypic features of CD4 and CD8 T cells in the spleen and thymus are comparable [34]. After the sensitizations, these mice were challenged with 0.5% DNFB five days after the last sensitization (on day 6; Fig. 1A, upper). These mice showed delayed type hypersensitivity with a single peak at 48 h after the challenge. The sensitized ROG Tg mice showed decreased ear swelling in comparison to the wild type $ROG^{+/+}$ mice, and the sensitized $ROG^{-/-}$ mice showed an increased ear swelling (Fig. 1A). These results indicate that ROG negatively regulates DNFB-induced CHS.

The infiltration of inflammatory cells was evaluated by histological analyses. Figure 1B shows that the levels of edema in the dermis were apparently different among the three groups, while the thickness of the inflamed epidermis (indicated by triangles; Fig. 1B) was similar among these three groups. There were similar numbers of infiltrating mononuclear cells and polymorphonuclear cells in the inflamed skin (Fig. 1C). Immunofluorescent staining was performed to assess the infiltration of $CD8^+$ T cells into the epidermis, and that of $CD4^+$ T cells into the dermis (Fig. 1D). The localization and the number of both infiltrating $CD8^+$ T cells and $CD4^+$ T cells were similar among the wild type $ROG^{+/+}$, ROG Tg and $ROG^{-/-}$ mice (Fig. 1D and E). FACS analyses of the single cells suspended from inflamed ear infiltrates showed no difference with regard to the percentage of $CD4^+$ or $CD8^+$ T cells among the three groups (data not shown).

3.2. Evaluation of the function of $CD8^+$ T cells from ROG Tg and $ROG^{-/-}$ mice during the elicitation phase of CHS

Since the effector phase of CHS is mediated mainly by $CD8^+$ T cells [5–11], and ROG is highly expressed in CD8 T cells [33], we assessed the function of CD8 T cells from ROG Tg and $ROG^{-/-}$ mice during the elicitation phase of CHS. The $CD4^+$ and $CD8^+$ T cell profile in regional lymph nodes and the activation status were assessed after DNFB challenge. The percentage of $CD4^+$ T cells and $CD8^+$ T cells in the left cervical lymph nodes did not show any difference among the wild type $ROG^{+/+}$, ROG Tg and $ROG^{-/-}$ mice, nor did the expression of surface markers, CD25 and CD69 on $CD8^+$ T cells (data not shown). The function of $CD8^+$ T cells in the regional lymph nodes was then assessed. $CD8^+$ T cells prepared from the left cervical lymph nodes of the DNFB-challenged mice were stimulated with 100 μg/ml of dinitrobenzene sulfonic acid (DNBS) with irradiated syngeneic spleen cells for 72 h, and the ability of antigen-specific $CD8^+$ T cells to produce IL-2 and IFN-γ was evaluated. The levels of IL-2 and IFN-γ in the culture supernatants were similar among the wild type $ROG^{+/+}$, ROG Tg and $ROG^{-/-}$ $CD8^+$ T cells (Figs. 2A and B, respectively). A CTL assay was conducted using EL-4 cells cultured with DNBS as the target to evaluate the cytotoxic activity of $CD8^+$ T cells in the regional lymph nodes of the DNFB-challenged inflamed ears, and no obvious difference was noted among the wild type $ROG^{+/+}$, ROG Tg and $ROG^{-/-}$ $CD8^+$ T cells (Fig. 2C). An adoptive transfer experiment was performed to further evaluate the function of hapten-primed $CD8^+$ T cells, and the adoptively transferred $CD8^+$ T cells from the wild type $ROG^{+/+}$, ROG Tg and $ROG^{-/-}$ mice elicited a similar level of ear swelling with or without DNFB sensitization after the transfer (Figs. 2D and E). These results indicate that the attenuating effect of ROG in the CHS may not be mediated by $CD8^+$ T cells.

3.3. Evaluation of serum antibody titers and mast cell degranulation in DNFB-treated ROG Tg and $ROG^{-/-}$ mice

The serum total IgE levels were measured on day 9 after sensitizing mice with DNFB three times (day 0, 1 and 7). The level of serum total IgE in the $ROG^{-/-}$ mice was higher than that of wild type mice (Fig. 3A). The levels of dinitrophenol (DNP)-specific IgG1 in the serum of ROG Tg mice were lower

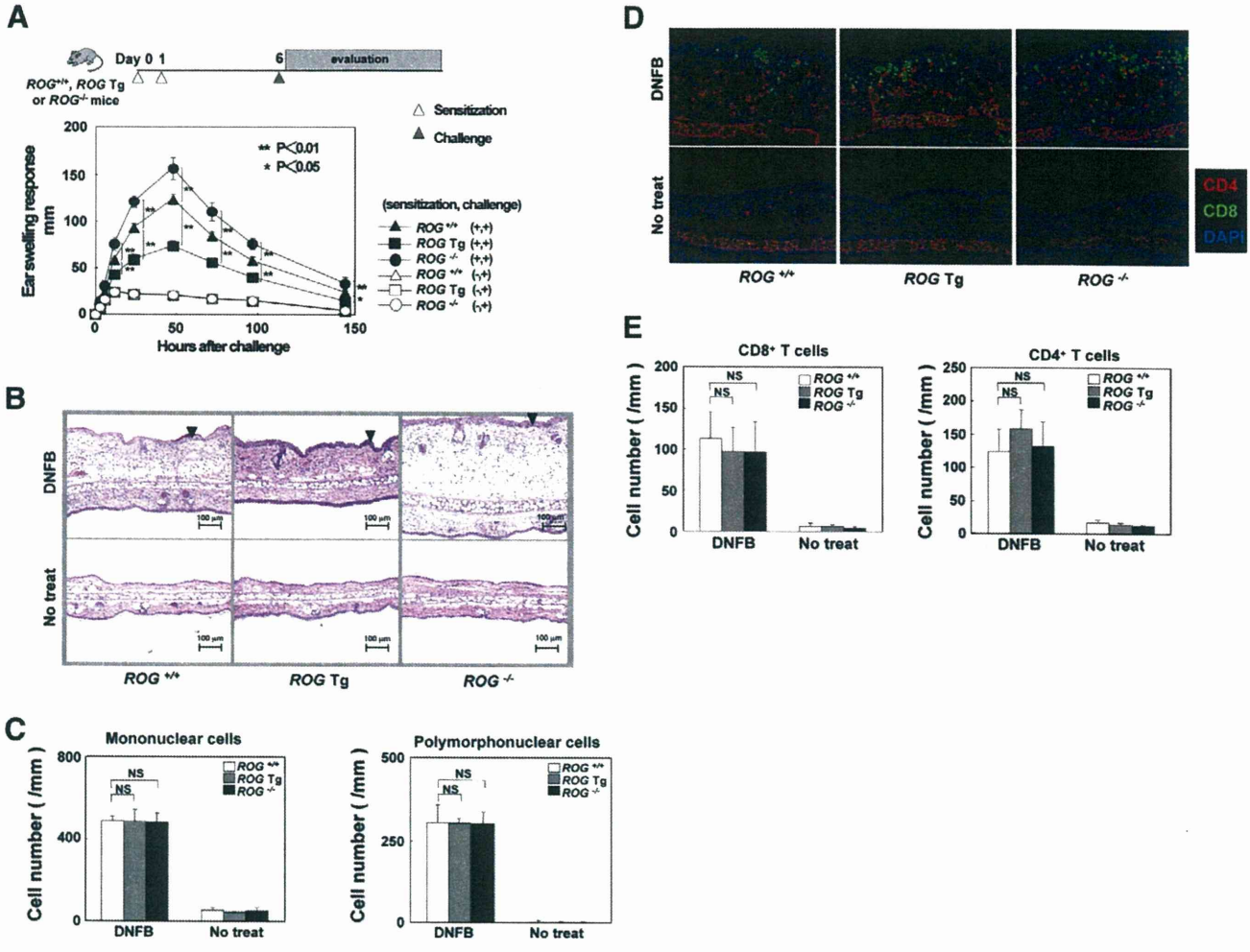

Figure 1 Ear swelling reactions and histological analysis in wild type mice, ROG Tg mice, and ROG$^{-/-}$ mice treated with DNFB. (A) After sensitization on days 0 and 1, mice were challenged in their left ear on day 6. Subsequently, the thickness of the ear was measured by a micrometer gauge. Negative controls were challenged but not sensitized. The data shown are representative of five experiments. (B) The left pinnae were excised 48 h after challenge and stained with hematoxylin–eosin for histological analyses. (C) The infiltrating mononuclear cells or the polymorphonuclear cells were counted by observation of 5 fields in each group. (D) Immunohistochemistry of the challenged ear tissues. CD8$^+$ T cells are shown in green, and CD4$^+$ T cells are shown in red by immunofluorescence. (E) The number of infiltrating CD8$^+$ T cells or CD4$^+$ T cells in each group is shown. A total of 8 fields were observed for each group. The mean values with their SD are indicated. The data shown are representative of five experiments. NS: not significant.

than those of the wild type, whereas those of the ROG$^{-/-}$ mice were higher than the wild type mice (Fig. 3B). The serum levels of DNP-specific IgG2a and IgG2b in these three groups were similar (data not shown).

May–Grunewald Giemsa staining of the ear pinnae was used to examine the mast cells in the inflamed skin tissue (Fig. 3C). The staining indicated that mast cells were yet to be degranulated as blue cells filled with metachromatic granules, whereas degranulated mast cells were detected as hollow blue-edged cells. The total numbers of mast cells was not altered by DNFB treatment, and also was not influenced by the expression level of ROG (Fig. 3D). As expected, the frequency of the degranulated mast cells were more increased in the ROG$^{-/-}$ mice in comparison to that in the wild type mice, whereas that in the ROG Tg mice was decreased (Fig. 3E).

3.4. The transfer of serum from DNFB-sensitized mice replicated the CHS in ROG Tg and ROG$^{-/-}$ mice

The serum of DNFB-sensitized wild type ROG$^{+/+}$, ROG Tg and ROG$^{-/-}$ mice was transferred into wild type C57BL/6 mice, and the ear swelling responses were evaluated after DNFB challenge. Figure 4A shows that the ear swelling responses were biphasic, as reported previously in a mouse atopic dermatitis model [37]. With regard to the late phase reaction, the mice that received the serum from ROG Tg mice showed reduced ear swelling in comparison to the response in the mice that received the serum of wild type mice, whereas the mice that received the serum from the ROG$^{-/-}$ mice showed enhanced reactions (Fig. 4A, left panel). In addition, 10 μg of anti-DNP IgE or anti-TNP IgE antibodies were injected as positive and negative

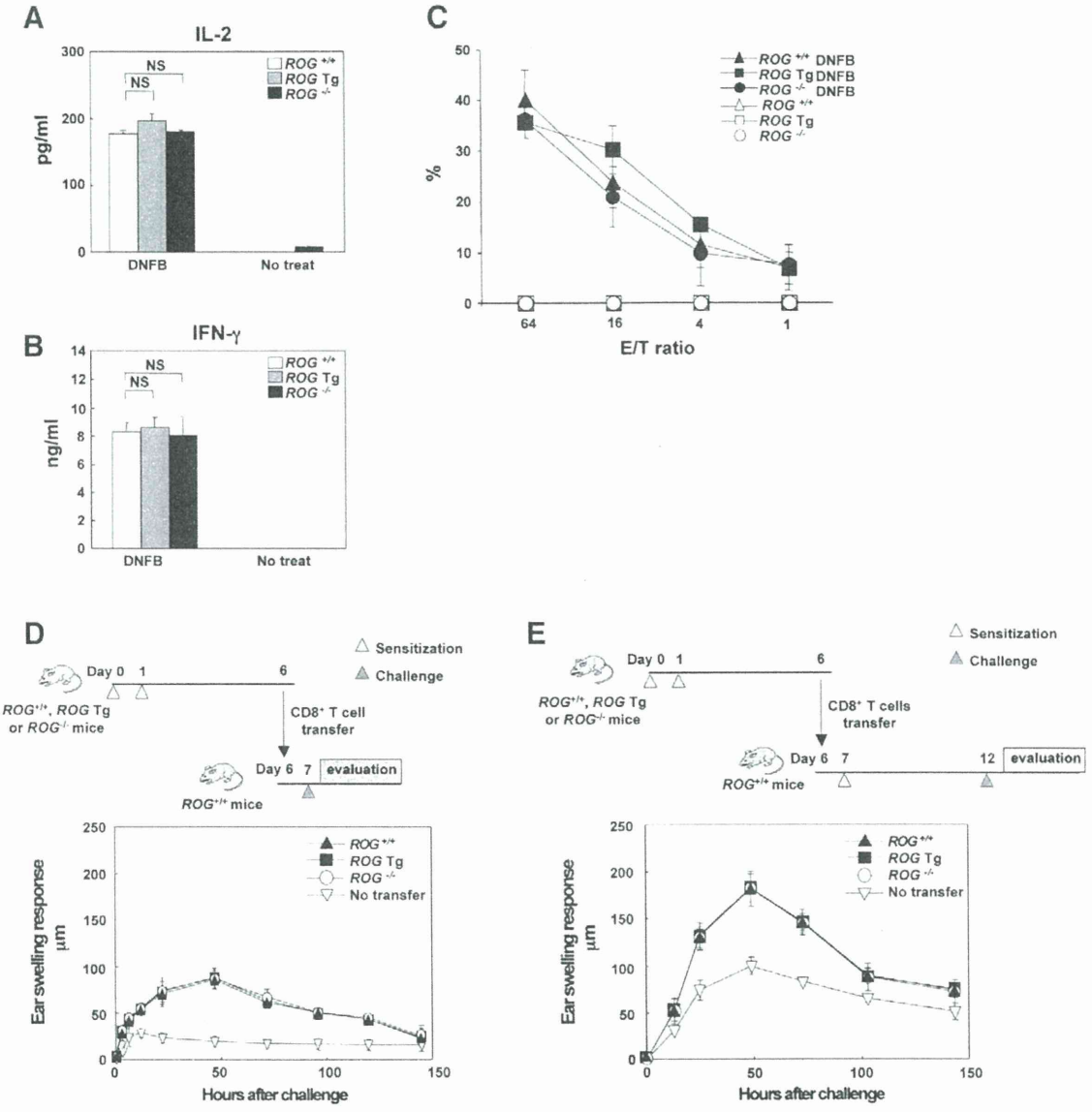

Figure 2 Evaluation of the functions of $CD8^+$ T cells from the ROG Tg and $ROG^{-/-}$ mice during the elicitation phase of CHS. (A–B) Cytokine production by $CD8^+$ T cells which were collected from the regional lymph nodes. The cells were stimulated with 100 μg/ml DNBS and irradiated splenic APCs from syngeneic mice *in vitro*. (C) A hapten-specific CTL assay was performed using DNBS-cultured EL-4 cells as targets to evaluate the function of $CD8^+$ T cells in the regional lymph nodes, which were recovered from DNFB-treated or non-treated mice on day 9 after being sensitized twice on their abdomen on days 1 and 2, and being challenged on the left ear on day 7. The $CD8^+$ T cells were restimulated with 3.8 ng/ml of IL-2 for 12 h *in vitro*. These cells were then assayed for cytolytic activity against EL-4 targets which had been cultured with 4 mM DNBS for 24 h. (D–E) The adoptive transfer experiment was carried out by transferring sensitized splenic $CD8^+$ T cells from the three different donor groups (the $ROG^{+/+}$, ROG Tg and $ROG^{-/-}$ mice) into the wild type syngeneic C57BL/6 recipient mice via a tail vein injection. Then in one experiment, the recipient mice were challenged on the following day, and the ear swelling responses were assessed (D). In another experiment, the recipient mice were sensitized once on day 7 and challenged on day 12, then the ear swelling responses were assessed (E). The mean values with their SD are indicated. NS: not significant.

controls, respectively. The mice that received anti-DNP IgE showed greater ear swelling than the mice that received the serum from $ROG^{-/-}$ mice, while the mice that received anti-TNP IgE showed decreased ear swellings in comparison to that observed in the mice that received the serum of ROG Tg mice (data not shown). Similar results were obtained in the acute phase reaction (Fig. 4A, right panel). The percentage of degranulated mast cells observed by May–Grunewald Giemsa staining were lower in the mice which received serum from the ROG Tg mice and higher in the mice that received serum from $ROG^{-/-}$ mice in comparison to that from wild type mice (Fig. 4B). These results indicate that antibody titers in the serum play an important role in the degranulation of mast cells in the skin, and also in the attenuating effect of ROG in the induction of CHS.

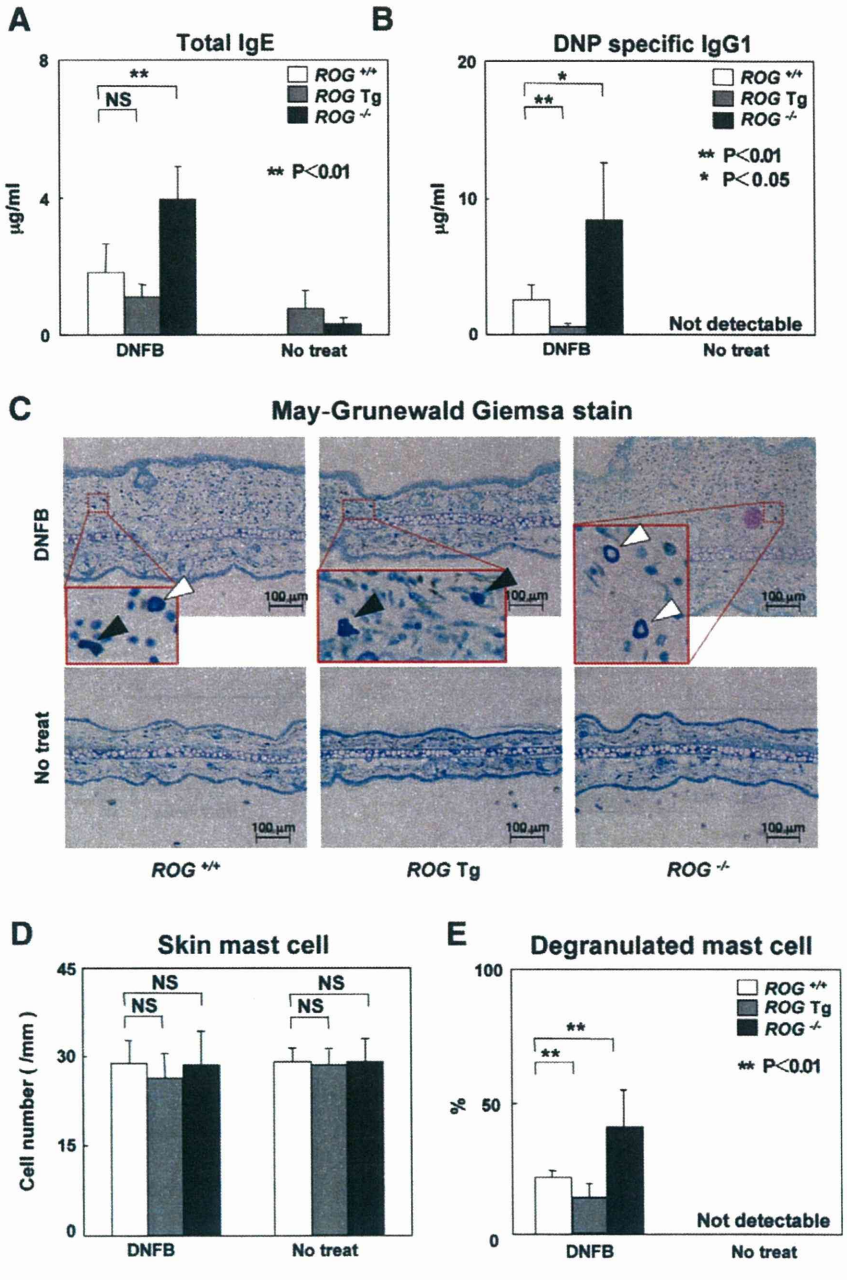

Figure 3 Evaluation of the serum antibody titers and mast cell degranulation in ROG Tg or ROG$^{-/-}$ mice. (A) The total IgE levels in the serum were measured by ELISA. The samples were taken on day 9 after sensitization on days 0, 1 and 7. (B) Serum IgG1 anti-DNP antibody levels were measured by ELISA. (C) May–Grunewald Giemsa staining of the ear pinnae, indicated mast cells that were yet to be degranulated as blue circles filled with metachromatic granules (indicated by black triangles), whereas degranulated mast cells (indicated by white triangles) were detected as hollow blue-edged circles. (D) The total number of the skin residential mast cells was counted. In each group, six microscopic fields from three mice were examined. (E) The percentages of the degranulated mast cells are shown. The percentage was calculated by counting the number of degranulated mast cells and the total number of mast cells in each field. The mean values with SD are indicated. NS: not significant.

3.5. The expression of ROG in CD4$^+$ T cells regulates the severity of CHS

To examine the contribution of ROG expression in CD4$^+$ T cells in the development of CHS, DNFB-sensitized CD4$^+$ T cells from wild type ROG$^{+/+}$, ROG Tg and ROG$^{-/-}$ mice were transferred into wild type mice, which were then challenged and evaluated for ear swelling responses. No CHS response was detected after challenging the mice on the following day after transfer of CD4$^+$ T cells (Fig. 5A). However, by sensitizing the mice transferred with DNFB-sensitized CD4$^+$ T cells once before challenge, the adoptively transferred CD4$^+$ T cells reconstructed CHS responses. As shown in Figure 5B, the mice that received the DNFB-sensitized CD4$^+$ T cells from